


Participation of extracellular signal-regulated kinases 1/2 in osteoblast and adipocyte differentiation of mesenchymal stem cells grown on titanium surfaces

Heitor F. Silva, Rodrigo P.F. Abuna, Helena B. Lopes, Marcelo S. Francischini, Paulo T. de Oliveira, Adalberto L. Rosa, Marcio M. Beloti 

Cell Culture Laboratory, School of Dentistry of Ribeirão Preto, University of São Paulo, Ribeirão Preto, SP, Brazil

Silva HF, Abuna RPF, Lopes HB, Francischini MS, de Oliveira PT, Rosa AL, Beloti MM. Participation of extracellular signal-regulated kinases 1/2 in osteoblast and adipocyte differentiation of mesenchymal stem cells grown on titanium surfaces. *Eur J Oral Sci* 2017; 00: 1–6. © 2017 Eur J Oral Sci

Osteoblasts and adipocytes coexist in the implantation site and affect the process of titanium (Ti) osseointegration. As extracellular signal-regulated kinases 1/2 (ERK1/2) are involved in osteogenesis and adipogenesis, the aim of our study was to investigate if the effects of Ti surface topography on osteoblast and adipocyte differentiation are modulated by ERK1/2. The experiments were conducted based on the effect of the ERK1/2 inhibitor, PD98059, on mesenchymal stem cells (MSCs) grown under osteogenic and adipogenic conditions on Ti with nanotopography (Ti-Nano) or on machined Ti (Ti-Machined). The results showed that, in general, ERK1/2 inhibition favored osteoblast and adipocyte differentiation of MSCs grown on Ti-Machined. In MSCs grown on Ti-Nano, ERK1/2 inhibition upregulated the expression of alkaline phosphatase and osteocalcin and reduced extracellular matrix mineralization. In terms of adipocyte differentiation, ERK1/2 inhibition elicited similar MSC responses to Ti-Nano and Ti-Machined, upregulating gene expression of adipocyte markers without affecting lipid accumulation. Our results indicate that, under osteogenic and adipogenic conditions, the responses of MSCs to Ti surface topography in terms of osteogenesis and adipogenesis are dependent on ERK1/2. Thus, a precise modulation of ERK1/2 expression and activity induced by surface topography could be a good strategy to drive the process of implant osseointegration.

Marcio Mateus Beloti, School of Dentistry of Ribeirão Preto, University of São Paulo – Av do Cafe s/n, 14040-904, Ribeirão Preto, SP, Brazil

E-mail: mmbeloti@usp.br

Key words: adipogenesis; implant; kinase; nanotopography; osteogenesis

Accepted for publication June 2017

The interaction between cells and titanium (Ti) is a key step in the process of implant osseointegration, and several surface characteristics may affect cell adhesion, proliferation, and differentiation, which ultimately dictate the formation of interfacial tissue. Among surface features, the topography, from microscale to nanoscale, has been shown to regulate cell responses to Ti (1–4).

The capacity of implants to modulate cell signals has been investigated, and the regulation of some pathways involved in osteogenesis has been associated with different surface topographies. The effect of an acid-etched, sandblasted, microstructured Ti surface on osteoblast differentiation involves canonical and non-canonical Wnt and transforming growth factor beta (TGF- β)/bone morphogenetic protein (BMP) signaling pathways (5, 6). The nanotopography of the Ti surface obtained by a simple, reproducible, and low-cost treatment with sulfuric acid/hydrogen peroxide (H₂SO₄/H₂O₂) induces osteoblast differentiation under either osteogenic or

non-osteogenic conditions (7, 8). Up to now, we have demonstrated that the osteogenic potential of this Ti surface involves its ability to inhibit the expression of microRNAs associated with the modulation of the BMP-2 signaling pathway (9). Furthermore, cells grown on this nanotopography synthesize larger amounts of endogenous BMP-2 and are more responsive to exogenous BMP-2 than cells grown on a machined surface (9, 10). Additionally, this surface triggers the α 1 β 1 integrin signaling cascade as the inhibition of this pathway reduces osteoblast differentiation induced by nanotopography (7).

In addition to Wnt, BMP, and integrins, the mitogen-activated protein kinase (MAPK) family is regulated by Ti surface topography. Specifically, the extracellular signal-regulated kinases 1 and 2 (ERK1/2) cascade may be modulated by Ti surface topographies exerting a direct effect on osteoblast differentiation (11). Extracellular signal-regulated kinases 1 and 2 act

as a switch for regulation of osteoblast and adipocyte differentiation by modulating runt-related transcription factor 2 (RUNX2) and peroxisome proliferator-activated receptor gamma (PPAR γ) expression and/or activity (12). While ERK1/2 phosphorylation is sustained during osteoblast differentiation, it is transient and decreases during differentiation of mesenchymal stem cells (MSCs) into adipocytes. In this scenario, surface topographies that regulate ERK1/2 expression and/or activity may induce a disruption of the balance between osteogenesis and adipogenesis, and consequently could affect Ti osseointegration.

Considering the osteogenic potential of nanotopography and the relevance of ERK1/2 for osteogenesis and adipogenesis, the aim of this study was to evaluate the participation of ERK1/2 in the interactions between MSCs and Ti using nanotopography (Ti-Nano) or machined Ti (Ti-Machined) during osteoblast and adipocyte differentiation.

Material and methods

Preparation of Ti surfaces

Discs of commercially pure grade 2 Ti, 12 mm in diameter and 1.5 mm thick, were polished using 320- and 600-grit silicon carbide, cleaned by sonication, and rinsed with toluene. Samples were treated with a blend of 10 N H₂SO₄ and 30% aqueous H₂O₂ (1:1, v/v) for 4 h at room temperature under continuous agitation to produce the surface nanotopography. Treated (Ti-Nano) and untreated (Ti-Machined) discs were rinsed with deionized H₂O, autoclaved, and air-dried. The surfaces were examined using a field emission scanning electron microscope (Inspect S50; FEI, Hillsboro, OR, USA) operated at 5 kV.

Isolation and culture of MSCs

Cells from male Wistar rats weighing 120–150 g were used in this study and all experiments were carried out according to the protocols approved by the Committee of Ethics in Research of the University of São Paulo (# 2015.1.163.58.5). Mesenchymal stem cells were obtained by flushing the femur medullary canals and were cultured in growth medium comprising minimum essential medium alpha (α -MEM; Gibco-Invitrogen, Grand Island, NY, USA) supplemented with 10% fetal calf serum (Gibco-Invitrogen), 50 μ g ml⁻¹ of gentamycin (Gibco-Invitrogen) and 0.3 μ g ml⁻¹ of fungizone (Gibco-Invitrogen). At 80% confluence, MSCs were enzymatically detached and used in the experiments described below. During the entire culture period, cells were kept at 37°C in a humidified atmosphere of 5% CO₂ and 95% air, and the medium was changed three times a week.

Effect of ERK1/2 inhibition on osteoblast differentiation of MSCs grown on Ti surfaces under osteogenic conditions

Cell culture: Mesenchymal stem cells were plated on Ti-Nano and Ti-Machined discs in 24-well culture plates at a cell density of 2×10^4 cells per well. Cultures were kept in osteogenic medium, which is growth medium

supplemented with 5 μ g ml⁻¹ of ascorbic acid (Gibco-Invitrogen), 7 mM β -glycerophosphate (Sigma-Aldrich, St Louis, MO, USA), and 10⁻⁷ M dexamethasone (Sigma-Aldrich), with or without (vehicle) 25 μ M PD98059 (Sigma-Aldrich), the ERK1/2 inhibitor, for periods of up to 21 d. The concentration of PD98059 was based on data from literature (13).

Gene expression of key osteoblast markers: Quantitative real-time PCR was carried out on day 10 to evaluate the expression of RUNX2, osterix (OSX), alkaline phosphatase (ALP), and osteocalcin (OC) genes. Total RNA was extracted with Trizol reagent (Invitrogen-Life Technologies, Carlsbad, CA, USA), according to the manufacturer's instructions, and 1 μ g of RNA was used to synthesize cDNA through a reverse transcription reaction (MMLV reverse transcriptase; Promega, Madison, WI, USA). Real-time PCR was carried out in a Step One Plus Real-Time PCR System (Invitrogen-Life Technologies) using Taqman PCR Master Mix (Applied Biosystems, Foster City, CA, USA). The relative gene expressions were normalized to β -actin expression and the real changes were expressed relative to MSCs grown on either Ti-Nano or Ti-Machined surfaces in the absence of PD98059 using the comparative threshold method ($2^{-\Delta\Delta C_t}$).

RUNX2 protein detection: At day 10, expression of RUNX2 protein was detected by western blotting. Cells were lysed in 500 μ l of lysis buffer containing 1 \times protease inhibitor mixture (Roche Applied Science, Indianapolis, IN, USA), and 25 μ M MG132 proteasome inhibitor (Roche Applied Science). Total protein of each sample (30 μ g) was subjected to electrophoresis in a denaturing 8.5% polyacrylamide gel and transferred to a Hybond C-Extra membrane (GE Healthcare Life Science, Piscataway, NJ, USA) using a semidry transfer apparatus (Bio-Rad Laboratories, Hercules, CA, USA). Membrane was blocked for 1 h in Tris-buffered saline plus 0.1% Tween 20 (TBS-T; Sigma-Aldrich) containing 5% non-fat powdered milk (Bio-Rad Laboratories). The RUNX2 protein was detected using rabbit polyclonal antibody to RUNX2 (1:3,000) (Cell Signaling Technology, Beverly, MA, USA) followed by secondary antibody, goat anti-rabbit IgG-horseradish peroxidase (HRP) conjugate (1:2,000, Santa Cruz Biotechnology, Santa Cruz, CA, USA). Mouse monoclonal anti-glyceraldehyde-3-phosphate dehydrogenase (GAPDH) (1:8,000, Sigma-Aldrich) was used as a control followed by the secondary antibody, goat anti-mouse IgG-HRP conjugate (1:2,000, Santa Cruz Biotechnology). Secondary antibodies were detected using the Western Lightning Chemiluminescence Reagent (PerkinElmer Life Sciences, Waltham, MA, USA) and the images were acquired using G:Box gel imaging (Syngene, Cambridge, UK). The expression of RUNX2 was quantified by counting pixels and normalized to expression of GAPDH.

Extracellular matrix mineralization: At day 21, cells were fixed in 10% formalin for 2 h at room temperature, dehydrated, and stained with 2% Alizarin Red S (Sigma-Aldrich), pH 4.2, for 10 min. The calcium content was measured using a colorimetric assay. First of all, 280 μ l of 10% acetic acid was added to each well and the plate was incubated at room temperature for 30 min under shaking at 400 rpm. The solution was heated at 85°C for 10 min, transferred to ice for 5 min, and centrifuged at 13,000 g for 15 min at room temperature. Then, 100 μ l of the

supernatant was mixed with 40 μl of 10% ammonium hydroxide and read at 405 nm in a plate reader (μQuant ; BioTek, Winooski, VT, USA); and the data were expressed as absorbance.

Effect of ERK1/2 inhibition on adipocyte differentiation of MSCs grown on Ti surfaces under adipogenic conditions

Cell culture: Mesenchymal stem cells were plated on Ti-Nano and Ti-Machined discs in 24-well culture plates at a cell density of 2×10^4 cells per well. Cultures were kept in adipogenic medium, namely growth medium supplemented with 10^{-6} M dexamethasone (Sigma-Aldrich), $0.5 \mu\text{M}$ 3-isobutyl-1-methylxanthine (Sigma-Aldrich), $10 \mu\text{g ml}^{-1}$ of insulin (Sigma-Aldrich), and 0.1 M indomethacin (Sigma-Aldrich), with or without (vehicle) $25 \mu\text{M}$ PD98059 (Sigma-Aldrich), for periods of up to 21 d.

Expression of genes for key adipocyte markers: Quantitative real-time PCR was carried out on day 10 to evaluate the expression of *PPAR γ* , adiponectin (*ADIPOQ*), and adipocyte protein 2 (*AP2*) genes, as described above.

Lipid accumulation: At day 21, cells were fixed in 10% formalin for 2 h at room temperature, washed with 60% isopropanol (Merck, Darmstadt, Germany), and stained with 0.3% Oil Red O (Sigma-Aldrich) for 10 min. Lipid accumulation was measured using a colorimetric assay. The Oil Red O incorporated was extracted by incubation with 100% isopropanol for 10 min under shaking at room temperature. Then, this solution was read at 500 nm in a plate reader (μQuant ; BioTek) and the data were expressed as absorbance.

Data analyses

The data are representative of three independent experiments using three sets of cultures established from different pools of rats. For each experiment, gene and protein expression were evaluated in triplicate ($n = 3$), and extracellular matrix mineralization and lipid accumulation were evaluated in quintuplicate ($n = 5$). The data were analyzed using the Mann–Whitney *U*-test to compare either cells grown on Ti-Machined with or without PD98059, or cells

grown on Ti-Nano with or without PD98059. The level of significance was established at $P \leq 0.05$.

Results

Topography of Ti surfaces

As expected, under scanning electron microscopy, Ti-Machined exhibited a smooth surface, while Ti-Nano showed a network of nanopores (Fig. 1A,B).

Effect of ERK1/2 inhibition on osteoblast differentiation of MSCs grown on Ti surfaces under osteogenic conditions

In general, on day 10, inhibition of ERK1/2 increased gene expression of osteoblast markers in cells grown on both types of Ti surfaces (Table 1), although this occurred mainly on Ti-Machined. The inhibition of ERK1/2 increased expression of *RUNX2*, *OSX*, *ALP*, and *OC* ($P = 0.001$ for all genes) in cells grown on Ti-Machined (Table 1). In cells grown on Ti-Nano (Table 1), inhibition of ERK1/2 did not affect expression of *RUNX2* ($P = 0.177$) or *OSX* ($P = 0.620$) genes and increased the expression of *ALP* ($P = 0.001$) and *OC* ($P = 0.001$) genes. On day 10, inhibition of ERK1/2 increased expression of RUNX2 protein in cells grown on Ti-Machined (Fig. 2A, $P = 0.017$), without affecting the expression of this protein in cells grown on Ti-Nano (Fig. 2B, $P = 0.315$). On day 21, inhibition of ERK1/2 did not affect extracellular matrix mineralization in cultures grown on Ti-Machined (Fig. 3A, $P = 0.330$) but did reduce extracellular matrix mineralization in cultures grown on Ti-Nano (Fig. 3B, $P = 0.001$).

Effect of inhibition of ERK1/2 on adipocyte differentiation of MSCs grown on Ti surfaces under adipogenic conditions

In general, on day 10, inhibition of ERK1/2 increased gene expression of adipocyte markers in cells grown on

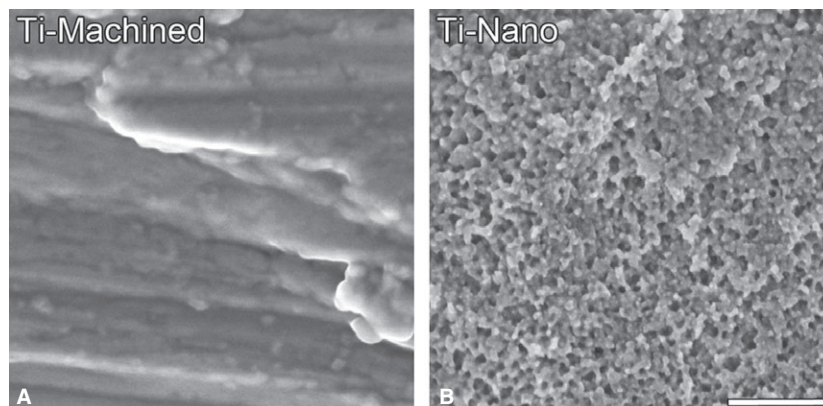


Fig. 1. High-resolution scanning electron micrographs of Ti-Machined (A) and Ti-Nano (B). Ti-Machined presents a smooth surface and Ti-Nano exhibits a network of nanocavities (B). Scale bar: 200 μm (both images).

Table 1

Gene expression and lipid accumulation in cells grown on Ti-Machined or on Ti-Nano in the presence or absence of the extracellular signal-regulated kinases 1/2 (ERK1/2) inhibitor, PD98059 (25 μ M)

	Gene expression							Lipid accumulation
	<i>RUNX2</i>	<i>OSX</i>	<i>ALP</i>	<i>OC</i>	<i>PPARγ</i>	<i>ADIPOQ</i>	<i>AP2</i>	
Ti-Machined	1.0 \pm 0.02	1.0 \pm 0.01	1.0 \pm 0.05	1.0 \pm 0.04	1.0 \pm 0.07	1.0 \pm 0.01	1.0 \pm 0.01	1.0 \pm 0.01
Ti-Machined +PD98059	1.7 \pm 0.02*	4.8 \pm 0.04*	2.5 \pm 0.07*	2.6 \pm 0.07*	2.7 \pm 0.07*	2.5 \pm 0.02*	3.1 \pm 0.02*	1.1 \pm 0.02
Ti-Nano	1.0 \pm 0.01	1.0 \pm 0.01	1.0 \pm 0.04	1.0 \pm 0.01	1.0 \pm 0.03	1.0 \pm 0.02	1.0 \pm 0.02	1.0 \pm 0.01
Ti-Nano +PD98059	0.9 \pm 0.01	1.1 \pm 0.01	1.5 \pm 0.01*	2.2 \pm 0.08*	1.7 \pm 0.02*	1.4 \pm 0.04*	1.6 \pm 0.04*	1.0 \pm 0.01

Values are given as fold change (mean \pm SD) on day 10.

The osteoblast markers runt-related transcription factor 2 (*RUNX2*), osterix (*OSX*), alkaline phosphatase (*ALP*), and osteocalcin (*OC*) genes were evaluated under osteogenic conditions, and the adipocyte markers peroxisome proliferator-activated receptor gamma (*PPAR γ*), adiponectin (*ADIPOQ*), and adipocyte protein 2 (*AP2*) genes, and lipid accumulation, were evaluated under adipogenic conditions.

*Statistically significant difference ($P \leq 0.05$).

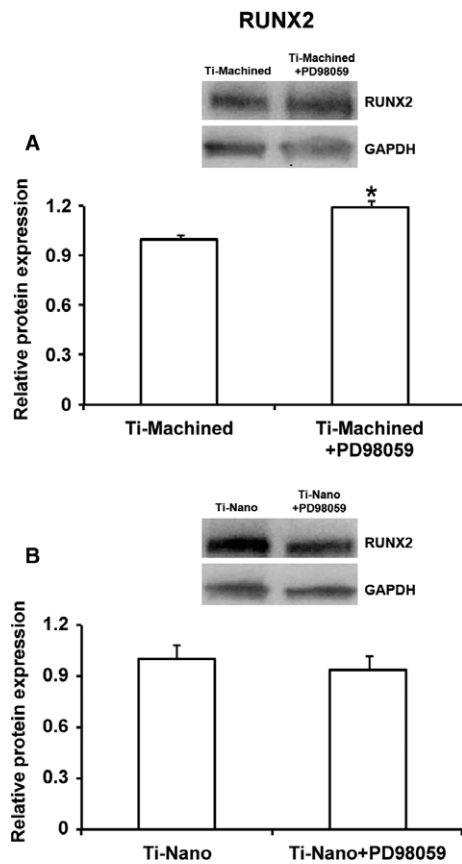


Fig. 2. Effect of inhibition of extracellular signal-regulated kinases 1/2 (ERK1/2) by PD98059 (25 μ M) on expression of runt-related transcription factor 2 (RUNX2) protein in cells grown on Ti-Machined (A) and Ti-Nano (B) under osteogenic conditions, on day 10. Inhibition of ERK1/2 increased expression of RUNX2 protein in cells grown on Ti-Machined (A), but did not affect expression of this protein in cells grown on Ti-Nano (B). The data presented are mean \pm SD ($n = 3$) and the asterisks indicate a statistically significant difference ($P \leq 0.05$).

both Ti surfaces (Table 1). The inhibition of ERK1/2 increased expression of *PPAR γ* , *ADIPOQ*, and *AP2* genes in cells grown on both Ti-Machined (Table 1,

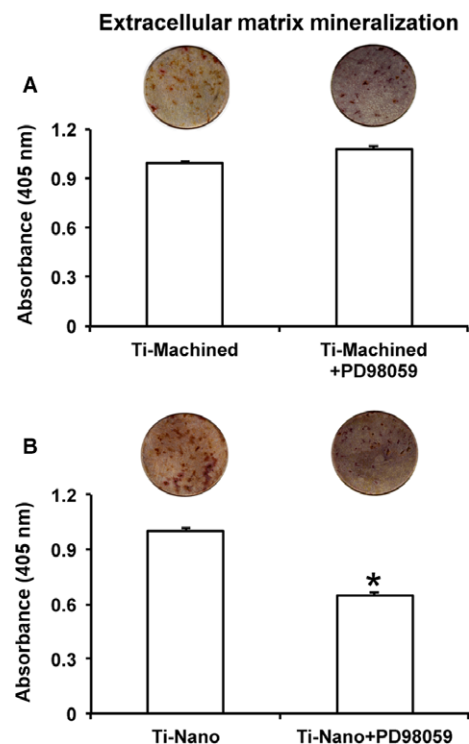


Fig. 3. Effect of inhibition of extracellular signal-regulated kinases 1/2 (ERK1/2) by PD98059 (25 μ M) on extracellular matrix mineralization in cultures grown on Ti-Machined (A) and Ti-Nano (B) under osteogenic conditions, on day 21. Inhibition of ERK1/2 did not affect extracellular matrix mineralization in cultures grown on Ti-Machined (A) but reduced extracellular matrix mineralization in cultures grown on Ti-Nano (B). Discs on the bars are representative of Alizarin Red S stains for each experimental condition. The data are presented as mean \pm SD ($n = 5$) and the asterisk indicates a statistically significant difference ($P \leq 0.05$).

$P = 0.001$ for all genes) and Ti-Nano (Table 1, $P = 0.005$, $P = 0.001$, and $P = 0.001$ for each gene, respectively). On day 21, inhibition of ERK1/2 did not affect lipid accumulation in cultures grown on both Ti-Machined (Table 1, $P = 0.083$) and Ti-Nano (Table 1, $P = 0.083$).

Discussion

This study aimed to evaluate the involvement of ERK1/2 in osteoblast and adipocyte differentiation of MSCs cultured on Ti-Machined and Ti-Nano. The results showed that, in general, MSCs grown on Ti-Machined are more responsive to these kinases, as inhibition of ERK1/2 enhanced osteoblast and adipocyte differentiation in a more noticeable way on Ti-Machined than on Ti-Nano.

Considering the process of implant osseointegration, osteoblasts and adipocytes constitute important cell populations because they coexist and interact in bone marrow (14, 15). These interactions should be considered in clinical situations because enhanced adipogenesis occurs in conjunction with decreased bone mineral density in animal models and in elderly and osteoporotic populations (16–18). In this scenario, ERK1/2 exert a key role as they can affect both osteogenesis and adipogenesis (12). Thus, our experimental design was based on the use of PD98059 to inhibit ERK1/2 in MSCs grown on Ti-Machined and Ti-Nano under osteogenic and adipogenic conditions. The inhibition of ERK1/2 favored the osteoblast genotype and phenotype of MSCs grown on Ti-Machined. In MSCs grown on Ti-Nano, inhibition of ERK1/2 generated more complex effects, upregulating *ALP* and *OC* genes without affecting expression of *RUNX2* and *OSX* genes. Additionally, expression of *RUNX2* protein was not affected, while reduced extracellular matrix mineralization was observed. Corroborating these findings, it has been shown that inhibition of ERK1/2 upregulates the gene expression of several osteoblast markers, such as *RUNX2*, *OSX*, and *OC* in the mouse pre-osteoblastic cell line, MC3T3-E1, grown on a sand-blasted and acid-etched rough Ti surface (11). One possible explanation for this positive effect is that ERK1/2 could prevent translocation of activated Smad to the nucleus, thus suppressing the BMP signaling pathway (19, 20). Consequently, the inhibition of ERK1/2 could potentiate the BMP signaling pathway, leading to increased expression of osteogenic markers. In contrast, the responses of human osteosarcoma MG63 cells to untreated, sand-blasted/acid-etched, and Ti plasma-sprayed Ti surfaces were not affected by inhibition of ERK1/2 (21). Although all studies used the same tool, PD98059, to inhibit ERK1/2, differences regarding cell source, commitment to the osteoblast lineage, and surface topography scale (either micro or nano) reveal the complexity of participation of ERK1/2 in osteoblast differentiation induced by Ti surface topography.

Under adipogenic conditions, the inhibition of ERK1/2 favored adipocyte differentiation of MSCs grown on both types of Ti surface, as evidenced by upregulation of *PPAR γ* , *ADIPOQ*, and *AP2* genes, without affecting the phenotype development, as evaluated by lipid accumulation. Despite the negative impact that this cell population may have on bone formation in contact with Ti implant (22), the effect of Ti surfaces on adipocyte differentiation and/or activity is underexplored, making comparisons of these results with data

from the literature difficult or even unfeasible. However, our findings are in agreement, to some extent, with the reduced ERK activity detected during adipogenesis in cultures of the ST2 mouse MSC line, the increased ERK phosphorylation associated with reduced adipocyte differentiation of mouse MSCs, and recovery of the propyl gallate-inhibiting adipogenic potential of human MSCs in response to ERK blocking (23, 24).

The osteogenic potential of Ti-Nano is related to its ability to modulate signaling pathways involved in osteogenesis, such as BMPs and integrins (7, 9, 10). Here, a possible additional mechanism involving the participation of ERK1/2 was investigated. Our results indicate that, under osteogenic and adipogenic conditions, MSC responses to Ti surface topography are dependent on ERK1/2. The inhibition of ERK1/2 enhanced osteoblast and adipocyte differentiation of MSCs grown on Ti-Machined. In addition, in MSCs grown on Ti-Nano, inhibition of ERK1/2 favored adipocyte differentiation and negatively affected the final event observed in an osteogenic culture, namely extracellular matrix mineralization. Thus, a fine-tune control of ERK1/2 expression and activity may be considered a good strategy to drive the balance between adipogenesis and osteogenesis on Ti surfaces and consequently to improve the process of implant osseointegration.

Acknowledgements – Roger Rodrigo Fernandes, Milla Sprone Tavares Ricoldi, and Fabiola Singaretti de Oliveira are acknowledged for technical assistance during the experiments. This work was supported by the State of São Paulo Research Foundation (FAPESP, Brazil) under the Grants # 2012/01291-6 and 2016/00182-0.

Conflicts of interest – The authors declare that they have no conflicts of interest.

References

- HOTCHKISS KM, REDDY GB, HYZY SL, SCHWARTZ Z, BOYAN BD, OLIVARES-NAVARRETE R. Titanium surface characteristics, including topography and wettability, alter macrophage activation. *Acta Biomater* 2016; **31**: 425–434.
- WANG T, WAN Y, LIU Z. Synergistic effects of bioactive ions and micro/nano-topography on the attachment, proliferation and differentiation of murine osteoblasts (MC3T3). *J Mater Sci Mater Med* 2016; **27**: 133.
- ZHAO G, ZINGER O, SCHWARTZ Z, WIELAND M, LANDOLT D, BOYAN BD. Osteoblast-like cells are sensitive to submicron-scale surface structure. *Clin Oral Implants Res* 2006; **17**: 258–264.
- SIMON M, LAGNEAU C, MORENO J, LISSAC M, DALARD F, GROSGOGÉAT B. Corrosion resistance and biocompatibility of a new porous surface for titanium implants. *Eur J Oral Sci* 2005; **113**: 537–545.
- OLIVARES-NAVARRETE R, HYZY S, WIELAND M, BOYAN BD, SCHWARTZ Z. The roles of Wnt signaling modulators Dickkopf-1 (Dkk1) and Dickkopf-2 (Dkk2) and cell maturation state in osteogenesis on microstructured titanium surfaces. *Biomaterials* 2010; **31**: 2015–2024.
- GALLI C, PASSERI G, RAVANETTI F, ELEZI E, PEDRAZZONI M, MACALUSO GM. Rough surface topography enhances the activation of Wnt/ β -catenin signaling in mesenchymal cells. *J Biomed Mater Res A* 2010; **95**: 682–690.
- ROSA AL, KATO RB, CASTRO RAUCCI LM, TEIXEIRA LN, DE OLIVEIRA FS, BELLESINI LS, DE OLIVEIRA PT, HASSAN MQ,

- BELOTI MM. Nanotopography drives stem cell fate toward osteoblast differentiation through $\alpha 1\beta 1$ integrin signaling pathway. *J Cell Biochem* 2014; **115**: 540–548.
8. DE OLIVEIRA PT, ZALZAL SF, BELOTI MM, ROSA AL, NÂNCI A. Enhancement of in vitro osteogenesis on titanium by chemically produced nanotopography. *J Biomed Mater Res A* 2007; **80**: 554–564.
 9. KATO RB, ROY B, DE OLIVEIRA FS, FERRAZ EP, DE OLIVEIRA PT, KEMPER AG, HASSAN MQ, ROSA AL, BELOTI MM. Nanotopography directs mesenchymal stem cells to osteoblast lineage through regulation of microRNA-SMAD-BMP-2 circuit. *J Cell Physiol* 2014; **229**: 1690–1696.
 10. CASTRO-RAUCCI LMS, FRANCISCHINI MS, TEIXEIRA LN, FERRAZ EP, LOPES HB, OLIVEIRA PT, HASSAN MQ, ROSA AL, BELOTI MM. Titanium with nanotopography induces osteoblast differentiation by regulating endogenous bone morphogenetic protein expression and signaling pathway. *J Cell Biochem* 2016; **117**: 1718–1726.
 11. ZHUANG LF, JIANG HH, QIAO SC, APPERT C, SI MS, GU YX, LAI HC. The roles of extracellular signal-regulated kinase 1/2 pathway in regulating osteogenic differentiation of murine preosteoblasts MC3T3-E1 cells on roughened titanium surfaces. *J Biomed Mater Res A* 2012; **100**: 125–133.
 12. JUNG HS, KIM YH, LEE JW. Duration and magnitude of extracellular signal-regulated protein kinase phosphorylation determine adipogenesis or osteogenesis in human bone marrow-derived stem cells. *Yonsei Med J* 2011; **52**: 165–172.
 13. LIU Q, CEN L, ZHOU H, YIN S, LIU G, LIU W, CAO Y, CUI L. The role of the extracellular signal-related kinase signaling pathway in osteogenic differentiation of human adipose-derived stem cells and in adipogenic transition initiated by dexamethasone. *Tissue Eng Part A* 2009; **15**: 3487–3497.
 14. SADIE-VAN GIJSEN H, CROWTHER NJ, HOUGH FS, FERRIS WF. The interrelationship between bone and fat: from cellular seesaw to endocrine reciprocity. *Cell Mol Life Sci* 2013; **70**: 2331–2349.
 15. ABDALLAH BM, KASSEM M. New factors controlling the balance between osteoblastogenesis and adipogenesis. *Bone* 2012; **50**: 540–545.
 16. LIU HY, WU AT, TSAI CY, CHOU KR, ZENG R, WANG MF, CHANG WC, HWANG SM, SU CH, DENG WP. The balance between adipogenesis and osteogenesis in bone regeneration by platelet-rich plasma for age-related osteoporosis. *Biomaterials* 2011; **32**: 6773–6780.
 17. DUQUE G. Bone and fat connection in aging bone. *Curr Opin Rheumatol* 2008; **20**: 429–434.
 18. DUQUE G, MACORITTO M, KREMER R. 1,25(OH)₂D₃ inhibits bone marrow adipogenesis in senescence accelerated mice (SAM-P/6) by decreasing the expression of peroxisome proliferator-activated receptor gamma 2 (PPARgamma2). *Exp Gerontol* 2004; **39**: 333–338.
 19. REILLY GC, GOLDEN EB, GRASSO-KNIGHT G, LEBOSY PS. Differential effects of ERK and p38 signaling in BMP-2 stimulated hypertrophy of cultured chick sternal chondrocytes. *Cell Commun Signal* 2005; **3**: 3.
 20. KRETZSCHMAR M, DOODY J, MASSAGUÉ J. Opposing BMP and EGF signalling pathways converge on the TGF-beta family mediator Smad1. *Nature* 1997; **389**: 618–622.
 21. SCHWARTZ Z, LOHMANN CH, VOCKE AK, SYLVIA VL, COCHRAN DL, DEAN DD, BOYAN BD. Osteoblast response to titanium surface roughness and 1,25-(OH)₂D₃ is mediated through the mitogen-activated protein kinase (MAPK) pathway. *J Biomed Mater Res* 2001; **56**: 417–426.
 22. TAKESHITA F, MURAI K, IYAMA S, AYUKAWA Y, SUETSUGU T. Uncontrolled diabetes hinders bone formation around titanium implants in rat tibiae. A light and fluorescence microscopy, and image processing study. *J Periodontol* 1998; **69**: 314–320.
 23. GE C, CAWTHORN WP, LI Y, ZHAO G, MACDOUGALD OA, FRANCESCHI RT. Reciprocal control of osteogenic and adipogenic differentiation by ERK/MAP kinase phosphorylation of Runx2 and PPAR γ transcription factors. *J Cell Physiol* 2016; **231**: 587–596.
 24. LIU GX, ZHU JC, CHEN XY, ZHU AZ, LIU CC, LAI Q, CHEN ST. Inhibition of adipogenic differentiation of bone marrow mesenchymal stem cells by erythropoietin via activating ERK and P38 MAPK. *Genet Mol Res* 2015; **14**: 6968–6977.